Available online www.unicrossjournals.com

UNICROSS JOURNAL OF SCIENCE AND TECHNOLOGY, UJOST

RESEARCH ARTICLE VOL. 3(3) SEPTEMBER, 2024 ISSN:2814-2233

Date Approved September 30, 2024 Pages 147 - 174

ANALYSES OF THE MICROCLIMATE AND GEOPHYSICAL PROPERTIES OF SOME FARMLANDS IN CENTRAL CROSS RIVER STATE FOR SUSTAINABLE AGRICULTURE USING INSITU DATA

Egor, A. O., Bisong, S.A., Osang, J. E.

Department of Physics, University of Cross River State, Calabar Nigeria

Email: atanegor@unicross.edu.ng

Abstract

Geophysical and metrological techniques were deployed to study the microclimate and soil properties of some locations chosen on the basis of their topography with the objective of engendering sustainable agricultural productivity. Climatic variables like sunshine, rainfall, evaporation, windspeed and temperature of the study location were monitored manually with sunshine recorder, standard rain gauge, class A evaporation pan, RM Young 81000 ultrasonic anemometer, and digital thermometer. This data was further corroborated with metrological data of 20 years from NIMET. The manually monitored data had average values of annual rainfall, sunshine, temperature, windspeed and evaporation of 317.13mm, 10.757(hours), 29.13(^{0}C), 1.9(m/s) and 46.39mm respectively. The Ground Penetrating Radar (GPR), a geophysical technique was used to determine the soil moisture content and porosity of the study area. The instrument used in data collection was MALA professional Explorer control unit (optical module) with antennae of frequency 200MHz. The data were collected at equal distance interval of 1m using a single offset method. The data obtained were analyzed using Rad-Explorer software version 1.4. The mean depth of 1.715 mm was selected for the determination of the velocity of the wave in the soil since the depth of the longest root of the crop can penetrate the soil is 1.5 mm. The findings of the study revealed that the mean value of soil water content and porosity of the soil at the hills of Ekabokom and Owakande are 0.2145m^3m^{-3} and 0.4866m^3m^{-3} while in Okuni and Obubra village it was 0.1168m^3m^{-3} and 0.3618m^3m^{-3} respectively. These results showed that the soil types of the areas are mainly loamy and sandy. Hence GPR has proven to be one of the most effective methods for electro geophysical soil characterization for the sustainable agricultural production. The soil moisture content was also measured *in situ* using a soil moisture content metre.

Keywords: Soil Moisture Content, Ground Penetrating Radar, Sustainable Agriculture, Microclimate, Windspeed, Temperature, Soil Porosity.

1.0 Introduction

Going through and assessing the harvest from most of the farms, it was observed that the harvests and outputs from the farms were significantly different, even when the hectarage and other factors such as agricultural inputs like fertilizer were applied equally on the soils. When every other factor like the viability of seedlings, adequate pre planting and post planting operations, pesticide, herbicides and fertilizer application is kept constant, yet the output across the farmland keep varying with the farmlands, then the microclimate of the farmlands is basically responsible.

An area's microclimate is its temperature, humidity, wind, turbulence, dew, frost, heat balance, and evaporation. Microclimatic conditions depend on these variables, and soil type has a significant impact on microclimates; sandy soils and other coarse, loose, and dry soils, for example, are subject to high maximum and low minimum surface temperatures. www.britannica.com/science/microclimate

Microclimates are essential for determining how a plant grows and thrives. Considerable temperature variations can be brought on by microclimates. For example, south-facing slopes and metropolitan areas tend to be warmer in warm microclimates. These zones may see faster growth and earlier blossoming for plants. In cold microclimates, the temperature is lower on north-facing hills and in shady places. Here, plants may develop more slowly and blossom later. Frost, on the other hand, is more common in low-lying areas and locations with inadequate air drainage. Plants that are susceptible to frost should be carefully picked for these areas. Soil moisture is influenced by microclimates. As an illustration: Sandy soils or exposed areas accelerate soil drying in arid microclimates. Here, drought-tolerant plants flourish.

Low-lying regions or areas with inadequate drainage tend to retain more moisture in wet microclimates. Only plants that are acclimated to moisture thrive. Windy microclimates increase transpiration, which can cause plants to dry out. Windbreaks (such as fences or hedges) can lessen this impact. Sunlight availability is determined by microclimates: Direct sunlight is necessary for plants to thrive, and in a full sun microclimate Plants that prefer shadow grow in microclimates that receive little sunlight. Humidity is higher in coastal regions and areas close to bodies of water. Humidity-adapted plants will thrive in that environment. Microclimates have an impact on soil microorganisms. Microbial activity is increased in warm, humid environments, which benefits plant nutrition availability.

It is common knowledge that agriculture is vulnerable to climate hazards, and that this has an impact on food security and farm livelihoods. To achieve the path of sustainable development, policy landscape adaptation to climate change is typically required.

The current meteorological conditions have a significant impact on agriculture. Agriculture is now increasingly vulnerable to climate hazards due to an increase in the frequency of extreme weather events such as floods, hailstorms, strong winds, heat waves, droughts, and cyclones. The productivity of agriculture is predicted to be severely impacted by climate change and global warming, primarily in tropical and subtropical regions. Rising temperatures have an impact on decreased crop output because they shorten crop duration and increase respiratory losses.

India's agricultural output demonstrates that the production of Kharif crops is more adversely affected by climatic variations. Since 1901, there has been an increase in the annual mean, maximum, and minimum temperatures of 0.61 °C/100 year, 1.0 °C/100 year, and 0.22 °C/100 year, respectively. Conversely, since 2000, the yearly precipitation has differed by almost 20% from the average. The amount of time that Rabi crops have to load their grains is also shortened by rising winter temperatures. As a result, the nutritional content of both crops is somewhat lost. Because of the permanent impacts of microclimate, a more varied and sustainable cropping strategy is required. A variety of laws and regulations have already been implemented to ensure profitable, sustainable agriculture. By addressing the unfavorable conditions surrounding the plants, microclimatic adjustments help to improve crop growth, production, and development.

Implementing such microclimatic changes in crop production is essential in the current climate of global warming and increased extreme weather events to manage the risks of extreme weather and boost crop productivity to increase food security and agriculture's sustainability under these changing climatic conditions Rukhsana, Alam, and Mandal (2021). In order to develop a non-destructive, intelligent method of measuring soil microclimate, this article will look at the geophysical method in addition to a few other approaches. Its precise results will help decision-makers make well-informed choices about crop selection and diversification, which, if implemented, will counteract the irreversible effects of microclimate. Additionally, the article will shed light on potential future agricultural practices in the Cross River State.

Ground Penetrating Radar (GPR) is one of the geophysical methods deployed in this research. The amount of water retained in the soil's pore spaces is referred to as soil moisture. According to Jung et al. (2010) and Mittelbach et al. (2012), soil moisture modifies the interactions between the atmosphere and the surface of the land, which affects the weather and climate. It is also necessary for defining the significant rainfall-runoff processes.

One essential ecosystem function that natural ecosystems provide is the maintenance of higher soil moisture levels; poor management could result in desertification (MEA, 2005a). The availability of soil moisture is necessary for natural cycling to take place, which is a requirement for primary production. The energy, carbon, and water cycles are connected to the terrestrial evapotranspiration process, which is controlled by soil moisture (Garten et al., 2009; Jung et al., 2010, Falloon et al., 2011).

Pielke et al. (2002) and Rhymer et al. (2010) claim that maintaining these associated ecosystem services increases natural ecosystem productivity and supports biodiversity.

Alkalinity, acidity, wilting point, field capacity, soil water potential, and soil matric potential are among the physical and chemical characteristics of a soil that affect its productivity and quality (Burk and Dalgliesh, 2008).

The soil's capacity to hold onto moisture has a major impact on the amount of water available in agroecosystems as well (Power, 2010). The soil's moisture serves as a binder, changing the structural integrity of the soil's hardness and stability. Water availability has a major impact on agricultural crop productivity, because soil moisture affects the chemical and biological processes that crop development and degradation involve.

Thus, in order to create site-specific management strategies that balance human activities with local environmental requirements, it is necessary to classify and monitor the soil qualities in the environment (Zhang et al., 2002).

The subsoil and intrinsic variability are inaccessible, making it challenging to collect soil data at the required spatiotemporal resolution. Determining the target dielectric constant's velocity and depth is crucial for this study since the dielectric constant of the host material is significant in GPR technology.

An electromagnetic (EM) technique often used by a Ground Penetrating Radar (GPR), is a geophysical method used to investigate the subsurface. Its objective is to describe the (GPR) wave's behavior at different hosting dielectric constants (Seyfried D et al., 2015). Electromagnetic waves and the signals they reflect off of subsurface structures are used in this non-destructive technique. GPR can be used to study a wide range of material, such as rocks, mud, ice, snow, water, and buildings. It is capable of recognizing cavities, fissures, underground items, and material differences. GPR method offers safety, probability, low cost, and non-destructivity. A thorough history of GPR is provided in.

In the past, geophysics has been applied in many fields, such as hydrology, engineering, and archeology. While the application of geophysics in agriculture has advanced significantly, it has received little attention. "Sustainable agriculture" refers to the way that agriculture and the environment are related, with an emphasis on food, fiber, and raw materials. It also highlights the need of managing a difficult environment while maintaining and enhancing the amount and quality of environmental resources. The region on this upper crust of the globe (also referred to as the "skin" of the planet) where agriculture is practiced is one of the complex systems in which the lithosphere, hydrosphere, and biosphere interact.

Alfred et al. (2000) estimated that the zone below the surface of the ground that is significant for agricultural research has a thickness of around 0.2 meters. Ground Penetrating Radar (GPR) is a geophysical method that will be used in this study to determine the kind of soil and its moisture content. Additionally, it seeks to validate the GPR technique as a substitute for other methods in CRUTECH for estimating soil moisture content. The survey results will also be used to ascertain the behavior of soil properties for engineering and agricultural purposes.

2.0 Theoretical Framework

Ground Penetrating Radar (GPR) is a geophysical technique that uses electromagnetic radiation to locate objects or interfaces buried below the surface of the earth Daniels, D.J. (2004). According to Conyers, L.B. (2003), a GPR system typically consists of three components: transmitting and receiving antennas, a control unit with a computer and associated software, and a display device. The transmitting antenna generates and sends earth-bound radar pulses, which are then either reflected, absorbed, or scattered by the objects buried below the surface. To improve the signal-to-noise ratio and accurately record the subsurface conditions, some of the radiations are emitted and travel before returning to the receiving antenna Cassidy N.J (2009).

In the VHS-UF region of the electromagnetic spectrum, GPRs are frequently used. Selecting the lowest frequency feasible will result in the best earth penetration depths. However, a high enough frequency must be employed in order to shorten the radar wavelength and make it possible to detect and resolve small objects, such as pipes.

Typically, cart-mounted radars run at a core frequency of 250MHz, while deep caves and mine shafts using frequencies as low as 20MHz, 500MHz and 1000MHz are occasionally employed for high resolution probing. A source antenna (Tx) is used to send radio wave pulses (between 100 MHz and 2.6 GHz) into the ground during a GPR inspection. The earth's electromagnetic characteristics cause the radio wave signal to be distorted as it travels through it Egor, *et al.*, (2023).

Subsequently, the reception antennas measure the radio wave signals at the boundaries where the subsurface electromagnetic characteristics abruptly change (Rx). Receiver antennas function as transducers by transforming the GPR signals they receive into electrical current because they are sensitive to the electric fields transmitted by radio waves. The voltage that results from the induced current is then digitally recorded. Lastly, as a function of time, GPR receivers measure the polarization and amplitude of incoming radio wave impulses. Because the raw data are eventually altered, radio wave transmissions undergo modifications due to earthly propagation, which affects their amplitude and polarization.

Using radio waves, GPR transmits data into the earth over relatively small distances and at speeds almost equivalent to the speed of light (C=3.0 x 108 m/s). Since GPR signals are sent from the transmitter antenna to the receiving antenna, their overall travel periods are extremely short. Up to a few hundred ns after the signal is created, the time series of a single GPR signal can be recorded. Data is recorded for a shorter amount of time after the transmitter generates the GPR signals (resulting in a shorter trip time) for GPR surveys intended to scan very close to the surface. Since shorts are only worn for a brief moment,

, The same transmitter-receiver pair and location can be used for many GPR measurements for a single short (sounding). Various models have been constructed to depict the various geological situations. The first model is a single profile that shows how electromagnetic waves propagate through various materials and how the wave is affected by electromagnetic properties. The second model is used to better comprehend the propagation of electromagnetic waves (reflected waves from radar-grams) through the geologic environment.

2.1 Velocity determination The wave's velocity is inversely proportional to the two-way travel time, reflector depth, and antenna separation (a, d).

$$V = \sqrt{\frac{4d^2+a^2}{TWTT}} \qquad (1)$$

The dielectric permittivity(k) is related to electromagnetic wave c by;

$$K = \left(\frac{C}{V}\right)^2 \qquad (2)$$

Where: K = dielectric permittivity,
C = Velocity of EM wave in m/n,
V = Velocity of the wave GPR analysis.

Available water content is determined in any farmland using the expression given by F.A. Organization. Corporate Document Repository (1985)

$AWC = 1000(\theta_{FC} - \theta_{WP})Z_r$

θ_{FC} is water content at field capacity, θ_{WP} is water content at wilting point Z_r − rooting depth in $mmmm$, AWC − available water content in mm Table 1a gives difference between the water content at field capacity and wilting point, which is the available water content for the uptake of the crop

2.2 Determination of soil water content

The water content of the soil was computed using Topp's equation as given by J. Davis and A. Annan, (1989)

$\theta = -0.053 + 0.0292k - 0.00055k^2 + 0.0000043k^3$

Where k is the dielectric permittivity of the soil and θ- the soil water content.

3.0 Physics of some of the Microclimatic Variables

3.1 **Temperature (^{0}C) and Sunlight**

The ozone layer is warm because it absorbs ultraviolet (UV) rays from the sun. The mesosphere is the layer above the stratosphere. The temperature decreases with height here just like it does in the troposphere. Heat transfer coefficient or film coefficient, in thermodynamics and in mechanics is the proportionality constant between the heat flux and the thermodynamic driving force for the flow of heat (i.e., the temperature difference, ΔT): (1) where: q = Amount of heat transferred (heat flux), W/m^2 (thermal power per unit area h = Heat transfer coefficient, W/(m^{2}K) ΔT = Difference in temperature between the solid surface and surrounding fluid area, K. It is used in calculating the heat transfer, typically by convection or phase transition between a fluid and a solid. The heat transfer coefficient has SI units in watts per square meter Kelvin: W/(m^2K).

3.2 Wind speed

The total inherent energy of the wind is determined by the following equation, Uquetan et. al. (2016)

$$P_{Total} = \frac{1}{2} PA\mu^3$$

Where:-

P_{TOTAL}: Total power (watts)

ρ: air density (1.225kg/m3)

A: Rotor Swept Area (m^2)

µ: wind speed (m/s)

Equation 2 is used for altitude varying wind speed and that relates the speed to the height assuming a low surface roughness. It provides an easy method for calculating the mean wind speed at a given height and power law equation is given as

$$\mu = \mu_i \left(\frac{z}{z_i}\right)^{1/7}$$

(3)

Where:-

$\mathcal{U}$= modified wind speed

$\mathcal{U}_i$ = wind speed data

z = height of turbine above ground level

z_i= normalize height.

There is increase in wind speed with increase in the height above the ground, due to the frictional drag of the ground, vegetation and buildings. It is important to put into consideration all these variables in order to harness the wind energy. The use of wind power for the supply of electricity broadens the energy base and reduces environmental pollution. It is particularly practical if it can be made economically competitive with conventional energy source. Amusan and sanusi (2007)

3.3 Rainfall

Rain is liquid water in the form of droplets that have condensed from atmospheric water vapor and then precipitated—that is, become heavy enough to fall under gravity. Rain is a major component of the water cycle and is responsible for depositing most of the fresh water on the Earth. The intensity and duration of rainfall are usually inversely related (high intensity storms are likely to be of short duration and low intensity storms are likely to have long duration), (Udo, et al., 2002), (Ryan, 2005). In view with (Afangideh et al., 2013; Udoimuk et. al. 2014),

$$Rainfall\ intensity \left(\frac{mm}{year}\right) = \frac{Annaul\ Rainfall\ amount}{Annual\ rainfall\ duration}$$

3.4 Geology and geomorphology of the study area

The area under study is in Central Cross River State of Nigeria. It is located between latitude 5º 45'N and 6º 28'N and longitude 8º 24'E and 9º 39'E of the Greenwich meridian (Eseme et al, 2002), at an elevation of 120.32m above sea level. with a tropical monsoon climate

This study was conducted in a farmland around Ekabokom Hillside in Ikom. The Ikom-Mamfe Embayment and Boki Geologic Environment are part of the region. The rainy season in IKOM is humid, muggy, and partially cloudy, whereas the dry season is heated, oppressive, and overcast. The average annual temperature fluctuates between 67°F and 89°F; it is rarely lower or higher than 63°F or 92°F. The Ikom-Mamfe embayment is the Northwest to Southeast splay part of the Northeast to Southwest trending Benue Trough. It extends laterally and covers 2,016 km 2 in western Cameroon Eseme, E., Agyingi, C. M. and Foba-Tendo, J. (2002). It is located in the lowlands between the Obudu Plateau and the Oban massif in The Ikom-Mamfe Embayment and the Boki Geologic Environment are included in the area.

The Northeast to Southwest trending Benue Trough's Northwest to Southeast splay portion is known as the Ikom-Mamfe embayment. It crosses 2,016 km 2 laterally in western Cameroon Pielke, R.A., Sr., Marland, G., Betts, R. A. Chase, T. N., Eastman, J. L., Niles, J. O., Niyogi, D., and Running, S.: (2002).

Its geography is somewhat undulating and it is situated in Nigeria's Cross River State, between the Oban massif and the Obudu Plateau (Fig. 1) Pielke, R.A., Sr., Marland, G., Betts, R. A. Chase, T. N., Eastman, J. L., Niles, J. O., Niyogi, D., and Running, S. (2002). Some settlements in Nigeria, primarily in the Cross River State, are included in this basin: Abi, Yakurr, Obubra, Ikom, and Etung (Fig. 1).

Underneath the Ikom-Mamfe basin, Precambrian basement rocks cover three significant Cretaceous lithostratigraphic units: the Asu River Group (ARG), Eze Aku Group (EAG), and Post-Semtonian Nkporo-Afikpo shales formation (NASF) (Odigi, 2010). Alluvial deposits can also be found in isolated locations in some of the Cross River flood plains, and Tertiary volcanic rocks such basalts and dolerites can occasionally be seen intruding into the Cretaceous sedimentary strata above them. Rhymer, C.M., Robinson, R.A., Smart, J., Whittingham, M.J., (2010). The Albian ARG, which are right on top of the Precambrian basement, are the oldest sedimentary rocks in the study area. They are mainly found in the eastern regions of the study area and range from being essentially non-marine to slightly marine (Fig.1). Impermeable shales comprise the sediments of the ARG. limestones with occasional sandstone intercalations, and ammonites.

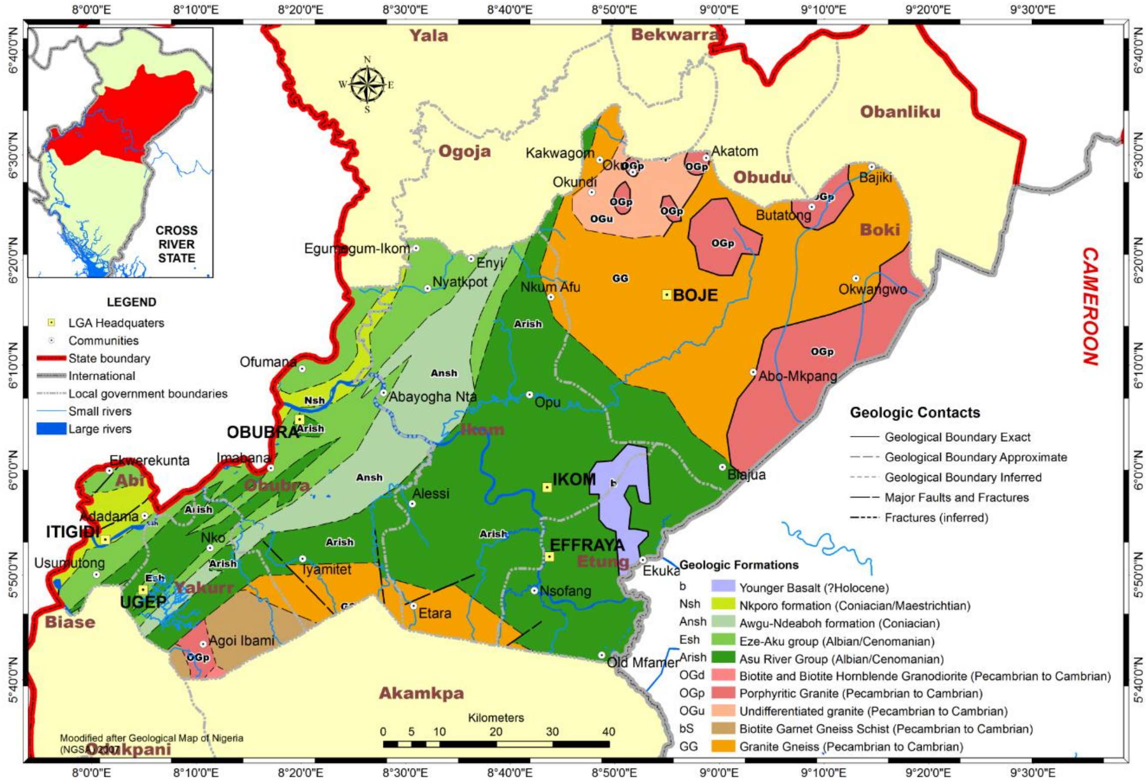

FIG. 1: Geological map of the study area

Source: Modified after Geological Map of Nigeria [Nigeria Geological Survey Agency (NGSA) (2006). Geological and mineral resources.]

4.0 Literature review

Ground penetrating radar (GPR) was used by George, A.M., Awak, E. A., and Abong, A.A. (2017) to measure the porosity, moisture content, and soil wetness in the farmlands of the Odukpani communities. Since the longest root of the crop can reach a depth of 1.8mm, an average depth of 2.075mm was selected to compute the wave velocity in the soil. The analysis's findings indicate that the soil at Odukpani measured 0.4556 mm3 and 0.1393 mm3, whereas the soil at Ekenkpon measured 0.12245 mm3 and 0.4606 mm3. These findings demonstrated that sandy and loamy soil types predominate in the region.

Consequently, in the context of precision agriculture, GPR has proven to be the most beneficial tool for hydro-geophysical soil characterisation. To determine the soil water content, the top 10 cm of a three-acre vineyard in California was exposed to Ground Penetrating Radar (GPR) ground wave technology. To ascertain the water content, GPR travel time measurements at 900 and 450 MHz were evenly spaced over a year. The estimate of the GPR water content is compared to the data on soil texture, gravimetric, and time-domain reflectometry.

The study's findings suggest that ground wave GPR technology can be used to quickly and non-invasively measure shallow water volume over wide areas. The 900MHz data showed volumetric water levels of 0.11, while the 450MHz data showed 0.017, with the largest inaccuracies being in very dry soils. In order to measure the spatial correlation of water content in a three-acre field as a function of sampling depth, season, vegetation, and soil moisture/texture, Grote, Anger, Kelly, Hubbard, and Rubin (2010) used the GPR. With the use of 450MHz and 900MHz antennas, the GPR data was collected.

Time domain reflectometry and soil texture data were used to find additional water content estimates. The results of the study demonstrated that the small-scale spatial correlations between soil texture and water content are frequently different, with deeper soil layers exhibiting a stronger link than shallower soil layers between soil texture and water content variation. Shallow-rooted vegetation minimizes regional variability in water content, while irrigation and precipitation increase geographical variability.

According to Bindlish, R., Jackson, T.J., Gasiewski, A., Klein, M., and Njoku, E.G. (2006), measuring soil moisture reliably and globally is difficult. Finding non-destructive methods that can be used to test moisture content directly and produce findings with higher resolution and accuracy is essential. The different tactics were divided into two groups by Murat RC (1972): indirect approaches and direct methods. Evett, S.R., Parkin, G.W., (2005), and Munoz-Carpena, R. (2012) state that measurements made using the direct approach are calibrated against other observable variables that change with soil moisture content. Weighing a soil sample both before and after drying will allow you to calculate the moisture content of the soil. The thermostat weight technique, also known as the gravimetric method, is the only direct approach; all other approaches fall under the category of indirect procedures. Except for remote sensing, all methods of determining soil moisture rely on the earth's surface.

5.0 Aim of the study

The purpose of this research project is to use geophysical, laboratory, and *in situ* methodologies to analyze some of the microclimatic factors, such as soil moisture content, temperature, wind, and evaporation, with the goal of enhancing the agricultural production of the studied area. Crop output and soil microclimate are directly correlated in that crop yield is sensitive to changes in the climate and microclimate. Osang et.al. (2017)

6.0 Objectives

I. To use a Ground Penetrating Radar (GPR) to obtain the moisture and water content of the soil in some farmlands in parts Central Cross River State.

II. To use the result of the survey to ascertain the behaviors of soil properties to agriculture.

7.0 Materials and methods

7.1 Data Source

The microclimatic data obtained manually through daily monitoring were aggregated into the monthly mean values of wind speed, rainfall, sunshine, temperature and evaporation. Annual climatic data of the same parameters were also collected from Ikom station of NIMET for a period of 20 years (2004-2023) and presented in table 4. Monthly Monitored microclimate of Ekabokom and Owakande recorded on table 3 and Table 5. Wind data were obtained from an anemometer mounted at the study area. A sunshine recorder was also was used to record daily sunshine. A rain gauge was also mounted at the study location to record the amount of rainfall. An evaporation pan was mounted at the at the study area to collect water and measure the amount lost to evaporation. All these measured parameters are recorded in table 5. Data on soil moisture content were obtained by measurement at some of the farmlands using a geophysics technique called the Ground Penetrating Radar (GPR) Recorded in table 7, table 9 and table 10. Furthermore, Insitu measurement of the soil moisture content was also done using a moisture meter which was inserted directly into the soil at 5m interval along the GPR profile line, the result is recorded on table 2. A hand auger was also used to collect soil samples at depths of 1m for analysis at the laboratory for some soil properties. Microclimate impact and variability was expressed using average, variance and standard deviation. Linear regression and principal component analysis was also used to establish the influence of rainfall, temperature, sunlight, wind speed, evaporation and soil moisture content (SMC).

The materials used for acquisition of GPR data, procedure for data collection and analysis are outline below: Single (constant) offset method was used in the survey. In this method, the two antennae; the transmitter and receiver are separated by a fixed or constant distance $a = 0.6\,m\ (in\ this\ case)$, the whole system is moved as a unit along the profile. Each profile was pegged at an (trace) interval of 1.0 m. The movement was done along these profiles in each location and data acquired at each pegged point. This interval was chosen for high resolution of the buried target.

The surveys were carried out at Ekabokom hillside and Owakande hillside in Ikom and Obubra local Government Areas respectively. The profile length at each of the locations varied between 70m to 110m

Acquisition software: Ground vision 2

Processing software: Geolitix GPR software

7.2 Processing procedure:

1. Raw data entered into the software in profile format.
2. Positioning: 90° to the vertical profile
3. Filtering applied: Time zero correction – to eliminate the travel time of the airwave shown on the data and set the actual time of first arrival to zero.
4. Gain applied: Energy decay – to improve the quality of the data
5. The hyperbola fixed in the radargram estimated the velocity of the wave as 0.06 m/ns.
6. This velocity gives the dielectric constant of K = 25
7. Depth of water concentration: 0.7 – 1.3 m as seen on the radargram (sky blue colour)

Table 1 Antenna properties for acquisition of GPR data

Frequency:	200MHz
Centre frequency:	200MHz
Resolution:	1.0m
Depth	7-12m
Number of samples	516
Trace number According to profile length	
Start time/end time	0/100ns
Antenna separation	0.6m
Background velocity	0.1m/ns
Air wave velocity	0.3m/ns

The following procedures were used to process the raw GPR data using the RadExplorer 1.4 program • 2. 1. DC removal: This method eliminates any constant signal components by changing the mean mode's start time to 0 ns and end time to 100 ns. • The vertical time scale's zero point is determined by the time adjustment routine, which sets time zero as the moment the wave really left the antenna. This was done in case the instrument didn't pick up the field's zero time. This repacking made sure that the profile's depths were accurate (Awak et al., 2017). Use 2D spatial filtering to determine the sample and trace sizes. This type of 2-D mean filter was applied to average the data inside the filter application window. Based on how long the profile was, the number of traces were determined.

8.0 Results and discussion

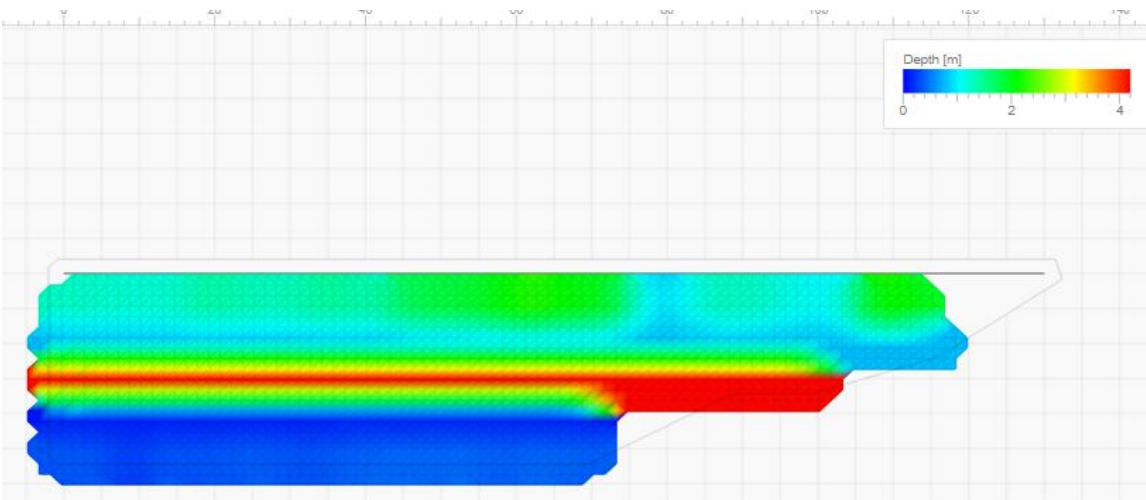

Figure 2a Transmitter Antenna

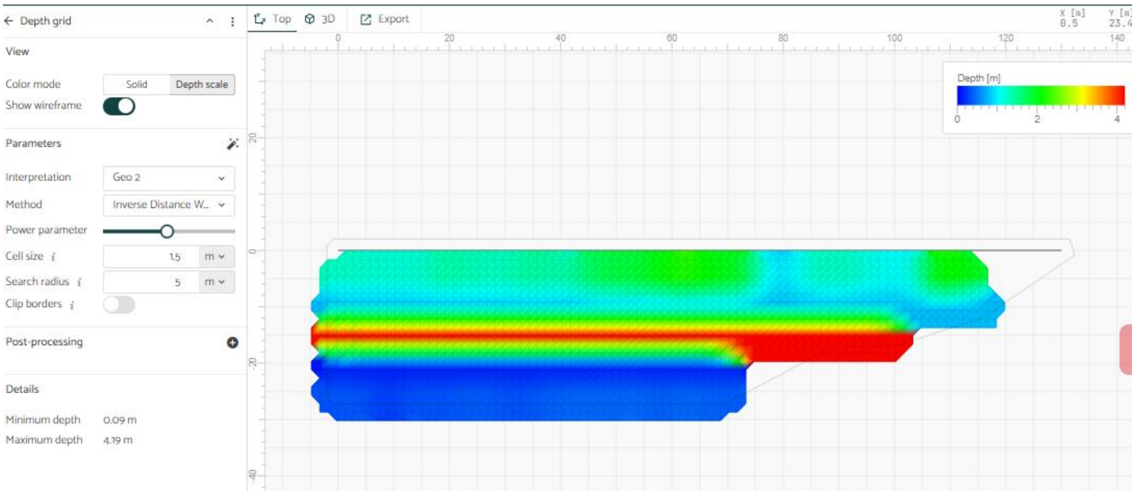

Figure: 2b Transmitter antenna

$$SMC = -0.053 + 0.0292K - 0.00055K^2 + 0.0000043K^3$$

$$SMC = 0.400438$$

TABLE 2: SMC data obtained at 5m interval along the GPR profile using soil moisture content meter with corresponding coordinates EKABOKOM HILLSIDE, IKOM

Interval (m)	Lg	Lt	SMC (%)
0	8.32665	5.1329	11.0
5	8.33264	5132937	13.3
10	8.33261	5.13984	11.0
15	8.3326	5.13301	11.4
20	8.3326	5.13301	9.9
25	8.33254	5.13309	14.5
30	8.33251	5.13313	13.1
35	8.33246	5.13316	13.4
40	8.33243	5.13323	29.6
45	8.33245	5.13324	16.6
50	8.33434	5.13353	9.6
55	8.33239	5.13331	11.2
60	8.33434	5.13353	9.7
65	8.33232	5.13338	25.5
70	8.33229	5.13341	10.5
75	8.33228	5.13345	10.6
80	8.33224	5.13349	8.8
85	8.33222	5.13326	16.3
90	8.3322	5.13357	12.1
95	8.33148	5.13361	12.6
100	8.33215	5.13364	17.7

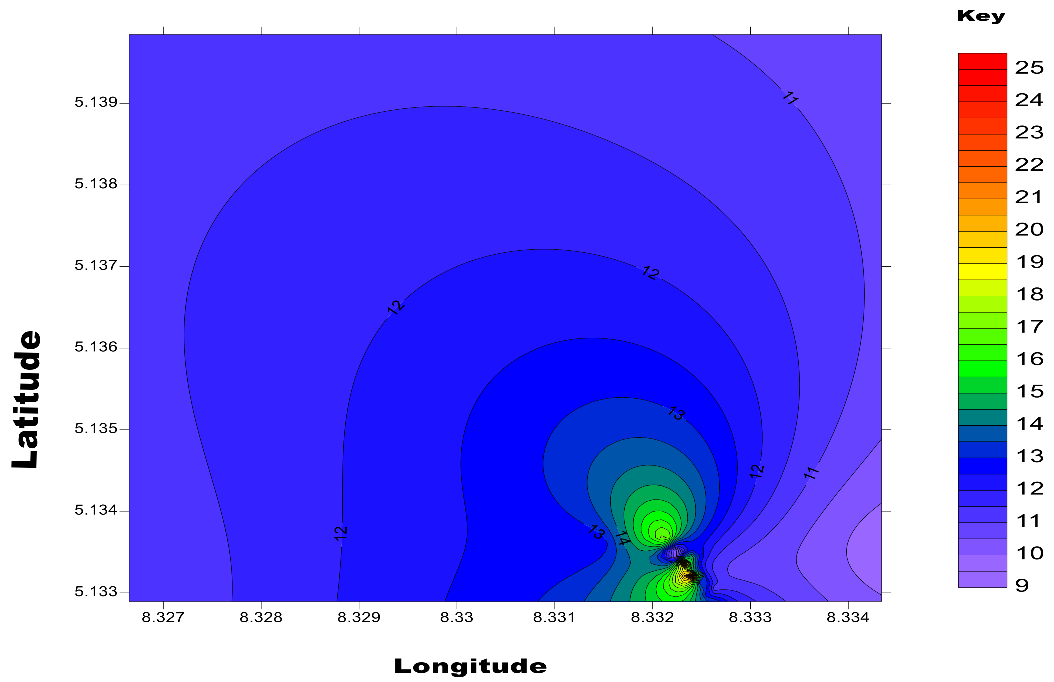

Figure3b: 2D SMC map of EKABOKOM HILLSIDE, IKOM at 5m interval from moisture meter along GPR profile length

Comparing Figure 2a and b, there is a positive correlation with the SMC from GPR data and that from moisture meter. Generally, the two figures show low SMC. In Figure 2b, the values of the SMC range from 9 – 13% and in figure 2a, the low SMC is shown in the regions of light blue colour all over the profile length

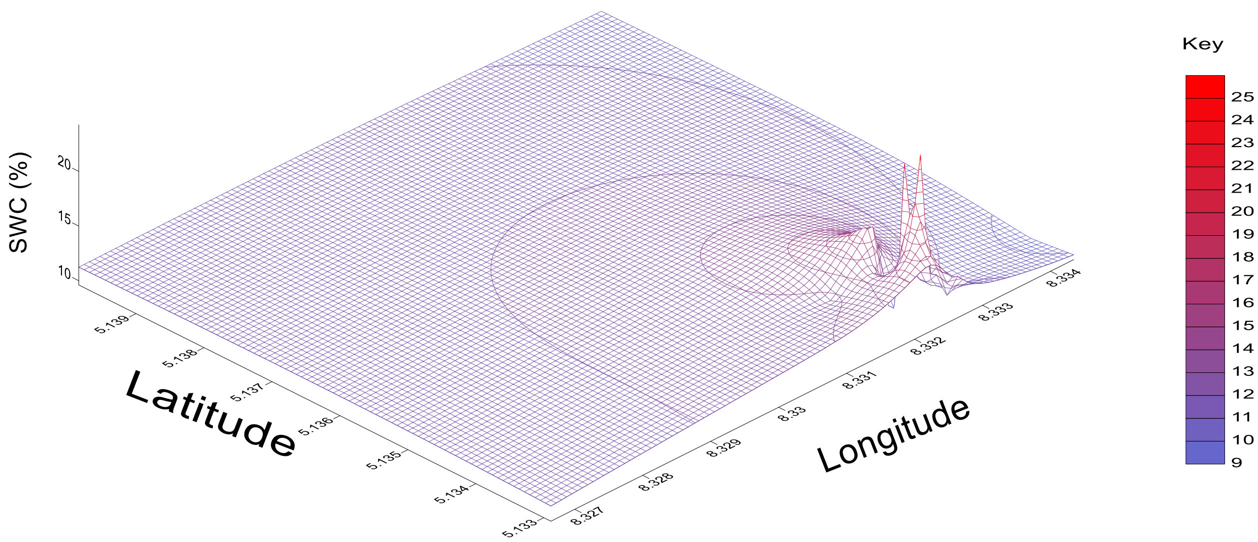

FIG. 3c: 3D SMC map of EKABOKOM HILLSIDE, IKOM.

Table 3. 2023 Observed monthly microclimatic parameters at EKABOKOM Hillside, IKOM

Month	**JAN**	**FEB**	**MAR**	**APR**	**MAY**	**JUN**	**JUL**	**AUG**	**SEP**	**OCT**	**NOV**	**DEC**	**Year**
Record High °C (°F)	42.11(108.7)	43.17(110.61)	43.17(110.61)	43.17(110.61)	42.11(108.7)	38.28(101.03)	35.10(95.27)	33.39(93.36)	36.16(97.2)	37.01(99.1)	38.25(101.03)	41.42 (106.77)	43.67(110.61)
Average high °C (°F)	37.43(100.45)	39.12(102.63)	38.47(101.97)	37.43(100.45)	35.37(96.03)	32.21(90.52)	30.36(87.01)	30.22(86.58)	30.53(87.67)	32.00(90.68)	34.28(94.06)	36.21 (97.54)	34.8(94.64)
Daily mean °C (°F)	31.53(88.93)	33.20(91.89)	33.56(92.77)	32.31(91.42)	31.09(88.14)	28.0(83.84)	27.21(81.36)	27.06(80.89)	27.33(81.73)	28.75(83.93)	30.29(86.7)	31.05 (88.07)	30.36(86.65)
Average low °C (°F)	21.70(71.35)	24.21 (75.58)	26.21(79.36)	26.09(79.32)	25.32(77.58)	23.73(74.71)	23.15(73.67)	23.02(73.44)	23.25(73.85)	23.63(74.53)	23.95(75.11)	22.87 (73.17)	23.97(75.15)
Record low °C (°F)	14.91(58.84)	18.11(64.6)	23.43(74.17)	23.43(74.17)	22.37(72.27)	21.3(70.34)	21.3(70.34)	21.3(70.34)	19.17(66.51)	21.3(70.34)	20.24(68.43)	18.11 (64.6)	14.91(58.84)
Average rainfall mm (inches)	15.0(0.59)	48.29(1.9)	115.36(4.54)	140.55(5.53)	180.35(7.1)	294.17(11.58)	520.94(20.51)	462.52(18.21)	459.88(18.11)	304.55 (11.99)	92.63(3.65)	13.11 (0.52)	220.61(8.69)
Average rainy days (≥ 0.3 mm)	3.78	11.24	20.05	23.34	25.18	27.79	32.44	30.6	30.7	28.28	18.01	3.39	21.23
Average relative humidity **(%)**	52.77	62.68	68.52	74.2	83.3	90.64	94.18	94.36	94.17	90.44	79.6	56.71	78.46
Mean monthly sunshine hours	12.26	12.15	11.71	11.59	11.2	10.45	9.92	9.63	9.85	10.8	11.63	12.02	11.1

Mean daily sunshine hours	5.4	5.2	3.5	4.5	4.4	4.3	1.8	1.6	2.0	3.4	4.5	5.7	3.8

Table 4. NIMET Ikom Station

S/N	YEAR	Annual rainfall (mm)	Temprature(°C)	Sunlight (Hours)	Windspeed(nus)	Evaporation(mm)
1	2004	1696.4	27.7	7.43	20.74	36.3
2	2005	1706.2	28.2	8.53	42	39.7
3	2006	2239.8	28.6	8.28	43.18	48.4
4	2007	2150.4	29.4	8.54	42.52	44.8
5	2008	1712.7	32.1	8.46	30.84	50.1
6	2009	1251.4	33.2	8.42	37.6	59.2
7	2010	2220.7	33.4	8.5	35.4	47.6
8	2011	1815.8	33.5 3	8.48	38.8	45.3
9	2012	1523.9	33.7	8.26	44.2	45.5
10	2013	1781.6	33.5	10.56	42.84	48.4
11	2014	1816.3	33.8	10.34	43	45.8
12	2015	2373.1	33.4	10.4	45.5	45.6
13	3016	2354.7	33.5	10.48	47.32	46.5
14	2017	2737.9	33.7	9.45	47.74	46.4
15	2018	2398.7	34.2	34.2	44.9	44
16	2019	2640.2	33.4	10.1	48.8	49.6
17	2020	1532.5	33.3	58.4	51.2	58.4
18	2021	1698.6	33.6	10.04	52.6	59.6
19	2022	1762.9	33.5	10.36	48.2	60.1
20	2023	1806.4	33.8	10.48	52.86	60.4
	AVERAGE	1961.01	32.475	9.3105	43.012	49.085
	VARIANCE	160175.4	4.443026	0.984594	58.89202	48.06345

	STDEV	400.2192	2.107849	0.992267	7.674113	6.932781

Fig 5 Monthly Climatic Parameters monitored manually in the study area

S/N	**Monthly average value**	**Windspeed Vm (m/s)**	**Temperature(°C)**	**Sunshine (Hours)**	**Rainfall(mm)**	**Evaporation(mm)**
1	Jan	2.3	37.43	12.43	20.7	36.3
2	Feb	2.5	39.12	12.53	39.3	39.7
3	Mar	1.8	38.46	11.28	38.1	48.4
4	Apr	2.2	33.56	10.54	98.5	44.8
5	May	1.8	31.13	9.46	430.8	50.1
6	Jun	2.1	28.20	9.12	478.5	59.2
7	July	1.5	23.41	9.01	658.7	47.6
8	Aug	2.1	23.5 3	9.21	854.6	45.3
9	Sept	2.0	23.07	9.26	630.5	45.5
10	Oct	2.2	28.5	10.56	410.7	48.4
11	Nov	1.6	33.8	11.34	120.6	45.8
12	Dec	1.9	35.4	12.14	25.2	45.6
	AVERAGE	1.9	29.13	10.75	317.13	46.39

Table 6. Water content values for different USA soil type by B.K. Bellinham (2009)

Soil Type (USA soil texture claasfication)	**Soil water characteristics (m^3m^{-3})**		
	θ_{FC}	θ_{WP}	$-\theta_{WP}$

Sand	0.120	0.040	0.080
Loamy sand	0.140	0.060	0.080
Sandy loam	0.123	0.100	0.130
Loam	0.260	0.120	0.140
Silt loam	0.300	0.150	0.150
Silt	0.320	0.165	0.155
Sandy clay loam	0.330	0.175	0.156
Silt clay loamy	0.340	0.190	0.150
Silty clay	0.360	0.210	0.339
Clay	0.360	0.210	0.339

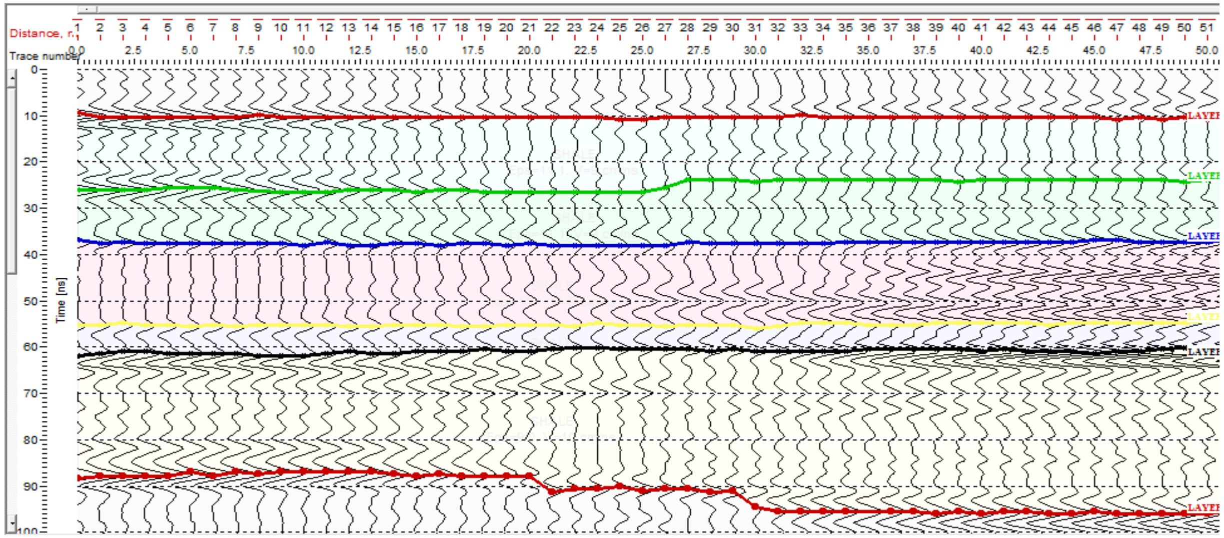

FIG.4a: Raw data

Location: EKABOKOM HILLSIDE

Profile length: 50m

Av. depth: 1.715m, av. twtt: 41.011 ns, V = 10.2 cm/ns, K = 8.4

In Fig.4a above, a profile length of 50m was carried out at the on the soil, and from the Raw data above, it is observed that there are several wiggles in each layer which entails water content.

Wiggles are due to the changes in dielectric constant that has caused deflection in the electromagnetic wave. So, the wiggles in the Raw data above are as a result of a deflection caused by water content present in the layer of the ground.

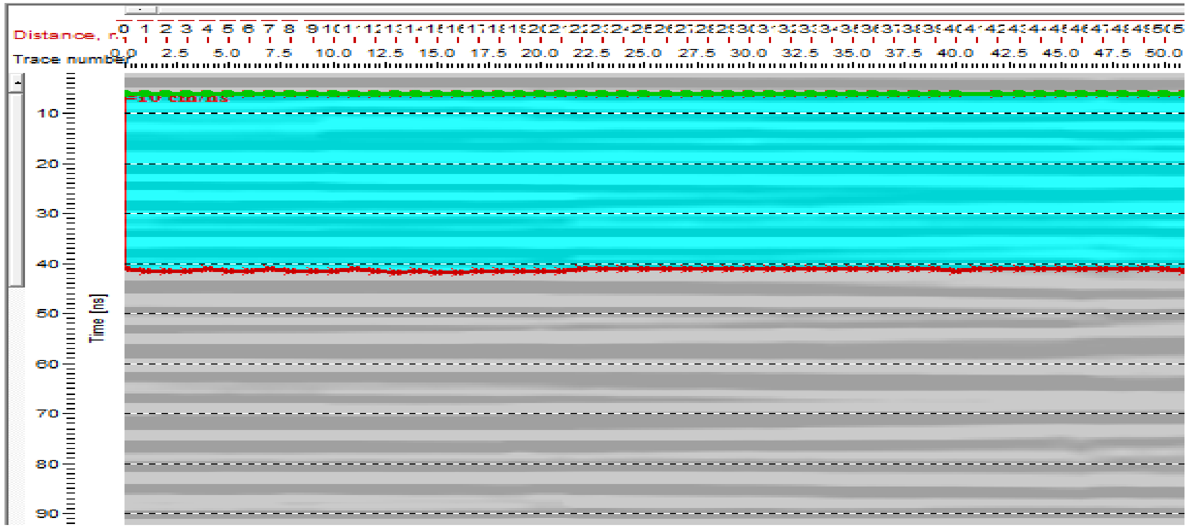

FIG. 4b: Model

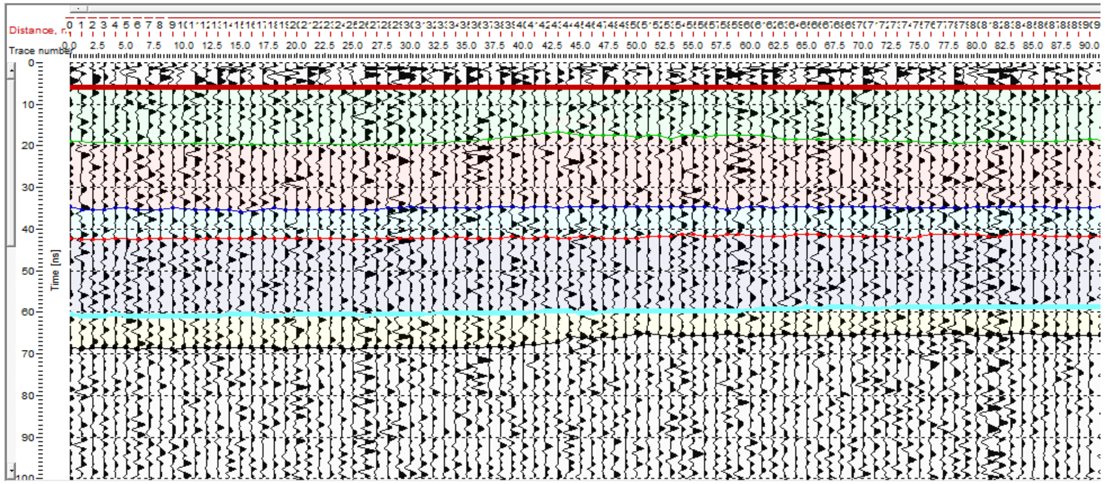

FIG. 4c: Raw data

Location: EKABOKOM 2

PROFILE DISTANCE: 50m

AVE. DEPTH: 1.715m AVE. TRAVEL TIME: 35.427ns V: 12.0cm/s K: 7.4

Table 7, showing Average depth (m), Average Two-Way Travel Time (ns), Velocity V(cm/s), Dielectric constant (K), and Soil moisture content
θ(m^3m^{-3})

LOCATION	Profile	Av. Depth	Av. TWTT	V	K	ϴ

	Length		(m)	(ns)	(cm/ns)	(m^3m^{-3})
EKABOKOM	110	1.715	41.011	10.2	8.5	0.1439
EKABOKOM 2	100	1.715	35.427	12.0	7.4	0.1347
OKUNI	100	1.715	33.417	12.5	5.8	0.1087
OBUBRA VILLAGE	100	1.715	35.013	11.4	9.3	0.
OWAKANDE LOWLAND	100	1.715	32.625	13.0	8.4	0.1547
OWAKANDE HILL	100	1.715	33.317	13.5	6.8	0.0886

According to George, A.M., Awak, E. A., & Abong, A.A. (2017), soil water content and apparent permittivity K are related by Topp's equation. The chart above shows that the average depth of all the profiles is 1.715 meters; nevertheless, it is crucial to remember that the maximum length of any root is approximately 1.5 meters. Because we are functioning on the soil moisture content, we usually increase the distance in order to sort for larger water content in that location.

It is evident from the values of the soil moisture contents acquired from the various sites that the farmland has a larger soil moisture content than the others, which makes it the perfect place for vegetation and agricultural activities.

The overall dielectric constant and the amount of soil moisture content in each layer, which are impacted by the soil type, both indicated that the research region had loamy soil based on the range of values in my data. Loamy soil has a high water-holding capacity and an ability to release excess water. Any leftover water falls downward because the particles permit unhindered drainage following irrigation or rain. Loamy soil does not easily crack when it dries out, thus plant roots are not in danger.

Table 8: Soil water contents for various soils expressed in different units.

Soil type	Available water content (AWC)		
	(mm/m)	(m^2m^{-2})	(%)
Sand	25 – 100	0.025 – 0.1	2.5 – 10
Loamy	100 – 175	0.1 – 0.175	10 – 17.5
Clay	175 – 250	0.175 – 0.25	17.5 – 25

(Source: FAO Cooperate Document Repository, 1985)

Table : Soil Moisture contents and Porosity of the Study Locations.

Study Location	Profile Code	Water content (m^3m^{-3})	Porosity (m^3m^{-3})
Ekabokom	0001	0.1125	0.3525
	0002	0.1211	0.3711
Owakande	0006A	0.1775	0.05117
	0007A	0.2510	0.4615

Table 10. RESULTS OF PAMETERS DERIVED FROM FIELD DATA

Study Location	Profile Code	Velocity	Dielectric Permitivity
		m/ns	K
Ekabokom	0001	0.12	6.5
Owakande	0002	0.10	7.1
Obubra	0006A	0.11	7.7

1. **Table 11: Ranges of water content that can support crop yield cultivated in the area**
   a. **by George, A.M, Awak, E. A. and Abong, A.A.(2017)**

2. Crop	3. Available water content (mm/m)	
	4. Sandy soil	5. Loamy soil
6. Cassava (1st year)	7. 40 – 64	8. 70 – 112
9. Cassava (2nd year)	10. 56 – 80	11. 98 – 140
12. Pumpkin	13. 80 – 120	14. 140 – 210
15. Maize (field corn)	16. 80 – 136	17. 140 – 238
18. Maize (sweet corn)	19. 64 – 96	20. 112 – 168
21. Cucumber	22. 56 – 96	23. 98 – 168
24. Sweet melon	25. 64 – 120	26. 112 – 210
27. Water melon	28. 64 – 120	29. 112 – 210
30. Tomato	31. 56 – 120	32. 98 – 210
33. Sweet pepper	34. 40 – 80	35. 70 – 140
36. Groundnut	37. 40 – 80	38. 70 – 140

9.0 Conclusion

One offset GPR approach was used to characterize the soil moisture content in the research region in a few farmlands in the central region of Cross-River State, at the hills of Ekabokom and Owakande, as well as lowlands. In Owakande, the average soil water content and porosity are 0.2145 m3 m-3 and 0.4866 m3 m-3, respectively, while in 0.1168 m3 m-3 and 0.3618 m3 m-3 elsewhere. The study finds that the majority of the study region is composed of loamy soil, which has little silt and sand particles in it. Loamy soil is mostly composed of sand, silt, and a small amount of clay. When dry, it has the consistency of concrete, and when wet, it turns into a sticky mess. For growing most plants and crops, loam soil can be preferable over other types of soil.

Because loam has about equal amounts of all three of these components, it is the ideal type of soil. The findings of this study demonstrated the need of monitoring soil moisture content for the purpose of planning precision agricultural programs and assessing the efficacy of water use. By optimizing crop yield and minimizing damage, this approach makes the best use of available water and land resources by adjusting soil moisture content (SMC). This is among the work's principal contributions.

Optimization helps the economy and the environment by increasing farm productivity and lowering irrigation costs. In conclusion, since loam soil, which best characterizes the soil composition for most farm crops, makes up the bulk of the region, some parts of the Central section of Cross River State may be appropriate for farming. Because of the soil's high moisture content, which guarantees that the soil's bearing capacity is not compromised, the soil is also seen to be great for civil engineering buildings and infrastructure.

Compliance with ethical standards

Acknowledgement

Special thanks go to the department of physics UNICAL for granting us access to their equipment. Nigeria Meteorological Agency NIMET for making the meteorological data available. The authors are also grateful to TETFUND for sponsoring this research under the institution based research (IBR) intervention.

Disclosure of conflict of interest

No conflict of interest exists between the authors

References

Afangideh, A. I., Ekpe, I. A., Offiong, R. A. (2013). Implications of changing rainfall pattern on building loss in Calabar: www.seahipub.org. retrieved 3:12pm, 9/11/2013

Alfred D., Daniel, J., & Reza E. M. (2000). Handbook of Agricultural geophysics. Taylor and Francis, Boca Roton, FL, USA.

Amusan J.A, Sanusi Y.K., and Fajinmi G.R., (2007). Determination of Annual Energy Capture potential for wind power system: A case study, *Research Journal of Applied Sciences* 2 (9), 927-930.

Bellinham, B.K. (2009). “Method for Irrigation Scheduling Based on soil moisture Data Acquisition" USA, United States Committee on Irrigation and Drain2009

Bindlish, R., Jackson, T.J., Gasiewski, A., Klein, M., Njoku, E.G., 2006. Soil Moisture mapping and AMSR-E validation using the PSR in SMEX02. *Remote Sens. Environ*. 103, 127-139.

Burk, L., Dalgliesh, N., (2008). Estimating Plant Available Water Capacity – a Methodology. CSIRO Sustainable Ecosystems, Canberra, 40p. [9] Power, A.G., 2010. Ecosystem services and agriculture: tradeoffs and synergies. *Phil. Trans. Roy. Soc.* B. 365, 2959-2971.

Cassidy N.J (2009). Ground Penetrating Radar data processing modelling and analysis: in ground penetrating modelling and application.

Conyers, L.B. (2003). Ground Penetrating Radar for archaeological, Rowman and Littlefield publishers Alta, Mira Press Lathon, MD, USA.

Daniels, D.J. (2004). Ground Penetrating Radar (GPR). The institution of engineering and Technology, London, UK: 1-4.

Davis JL, Annan AP. 1989. Ground-Penetrating Radar for High-Resolution Mapping of Soil and Rock Stratigraphy. Geophysical Prospecting, 37:531-551.

Davis, J. & Annan, A. (1989). "Ground penetrating radar for high resolution mapping of soil and rock stratigraphy." Geophysical Prospecting,37,531–551,1989.

Egor, A. O. (2023). Deployment Of Ground Penetrating Radar (GPR) Technique in the Determination of Soil Moisture Content of Parts of University Cross River State Soil for Precision Agriculture in South-South Nigeria. Department of Physics, Cross River University of Technology, Nigeria. *Journal of Contemporary Research (JOCRES).* VOL. 2 (1) ISSN:2814-2241.

Eseme E, Agyingi CM, Foba-Tendo J (2002) Geochemistry and genesis of brine emanations from Cretaceous strata of the Mamfe Basin, Cameroon. J Afr Earth Sci 35:467–476 [14] Benkhelil J (1982) Benue trough and Benue chain. *Geol Mag Niger* 119:115–168

Eseme, E., Agyingi, C. M. Foba-Tendo, J. (2002). Geochemistry and genesis of brine emanation from cretaceous strata of the Mamfe Basin, Cameroon, *J. Afr. Earth Sc.* 35:467-476 Doi: 10.1016/SO899-5362(2)00171-9.

Evett, S.R., Parkin, G.W., 2005. Advances in soil water content sensing: the continuing maturation of technology and theory. Vadose Zone J. 4, 986-991.

F.A. Organization. Corporate Document Repository, "Irrigation Water Management: Introduction to irrigation". Produced by National Resource Management and Environmental Department, 1985

Falloon, P., Jones, C.D., Ades, M., Paul, K., 2011. Direct soil moisture controls of feature global soil carbon changes: an important source of uncertainty. Glob. Biogeochemist. Cycles 25, GB3010.

Garten Jr., C.T., Classen, A.T., Norby, R.J 2009. Soil moisture surpasses elevated CO_2 and temperature as a control on soil moisture dynamics in a multi-factor climate change experiment. Plant. Soil 319, 85-94.

George, A.M., Awak, E. A. & Abong A.A (2017). Precision Agriculture using Ground Penetrating Radar (GPR): A case study of part of Odukpani Local Government area, Cross-River state, Nigeria.

Grote. K, Anger. C, Kelly. B, Hubbard. S & Rubin. Y. 2010. Characterization of Soil Water Content Variability and Soil Texture using GPR Groundwave Techniques. J. *Environ. Eng. Geophys.*, 15:93-110.

Jung, M., Reichstein, M., Ciais, P., Sheffield, J., Goulden, M.L., Bonan, B., et al., 2010. Recent decline in the global land evapotranspiration trend due to limited moisture supply. Nature 467, 951-954.

Mittelbach, H., Lehner, I., Seneviratne, S.I., Comparison of four soil moisture sensor types under field conditions in Switzerland. *J. Hydrol*. 430-431, 39-49.

Munoz-Carpena, R., 2012. Field devices for monitoring soil water content. Agricultural and Biological Engineering Department, University of Florida. BUL343.

Murat RC (1972) Stratigraphy and paleogeography of the cretaceous and lower tertiary in southern Nigeria. In: Dessauvagie TFJ, Whiteman AJ (eds) African geology. Ibadan Univ. Press, Ibadan, pp 251–266

Nigeria Geological Survey Agency (NGSA) (2006). Geological and mineral resources

Odigi MI (2011) Diagenesis and reservoir quality of cretaceous sandstones of Nkporo formation (campanian) southeastern Benue trough, *Nigeria. J Geol Min Res* 3(10):265–280.

Odigi MI, Amajor LC (2009) Geochemical characterization of cretaceous sandstones from the Southern Benue Trough, Nigeria. *Chin J Geochem* 28:44–54

Osang, J. E.[1], Uquetan, U. I.[2], Oko, P. E.[2], **Egor, A. O.[1]**, Ekwok, S. E.[3], and Ekpo, C. M.[2] (2017). Effect on pH Value of Rain Water and Soil pH in River State Nigeria Department of Physics, Cross River University of Technology, Calabar, Nigeria. *Elixir Environ. & Forestry* 110 (2017) 48174-48183.

Pielke, R.A., Sr., Marland, G., Betts, R. A. Chase, T. N., Eastman, J. L., Niles, J. O., Niyogi, D., and Running, S.: 2002, "The influence of land use change and landscape dynamics on the climate system relevance to climate change policy beyond the radiative effect of greenhouse gases". *Phil. Trans*. A 360, 1705-1719.

Power, A.G., 2010. Ecosystem services and agriculture: tradeoffs and synergies. *Phil. Trans. Roy. Soc. B*. 365, 2959-2971.

Rhymer, C.M., Robinson, R.A., Smart, J., Whittingham, M.J., 2010. Can ecosystem services be integrated with conservation? A case study of breeding waders on grassland. Ibis 152, 698-712.

Rukhsana, Alam, A., Mandal, I. (2021). Impact of Microclimate on Agriculture in India: Transformation and Adaptation. In: Rukhsana, Alam, A. (eds) Agriculture, Food and Nutrition Security. Springer, Cham. https://doi.org/10.1007/978-3-030-69333-6_3

Rukhsana, Alam, A., Mandal, I. (2021). Impact of Microclimate on Agriculture in India: Transformation and Adaptation. In: Rukhsana, Alam, A. (eds) Agriculture, Food and Nutrition Security. Springer, Cham. https://doi.org/10.1007/978-3-030-69333-6_3

Ryan, C. Rank(2005). "Bubble Resonance." The physics of Bubbles an Antibubbles, and all that retrieve2006-12-09

Seyfried, D. et al; (2015). Proceedings of SPIE, volume 4158, iii0 April to 2 May 2002. University of California, Santa Barbara, California.

Udo, S. O., Ani, O. E., Oduro-Afriye, K. (2002). Effect of moisture and bulk density on soil temperature. *Global Journal of pure and applied science* Vol. 8, No. 1, pp 125-132

Udoimok, A.B., Osang ,J.E., E.B., Usie P. O., Egor, A. O., Alozie, S. I.(2014). Empirical study of seasonal rainfall Effect in Calabar, Cross River State, Nigeria. *IOSR Journal of applied physics (IOSR* -JAP*) E* - ISSN: 2278-4861. Vol 5, Issue 5

Uquetan, U. I.[1], Amah, A. E[1], Igelle, E. I.[1], **Egor, A. O.[2]**, Ekpo, C. M. [2]. and Osang, J. E.[2] (2017). Effect of Traffic Density on Soil along Nwanga-Ekoi-Mfamosing Road Cross River State, Nigeria Department of Geography & Environmental Science, University of Calabar, Nigeria. *Elixir Environ. & Forestry* 110 (2017) 48162-48167.

Uquetan, U. I.[1], Igelle, E. I.[1], **Egor, A. O.[2]**, Inah, E. O.[1], Osang, J. E.[2], and Ekpo, C. M.[2] (2017). Impacts of Climate Variables on Water Yield in Ujama Okpauku River, Yala Lga, Cross River State, Nigeria Department of Geography & Environmental Science, University of Calabar, Nigeria. *Elixir Environ. & Forestry* 110 (2017) 48168-48173.

Zhang, R., Wienhold, B.J. The effect of soil moisture on mineral nitrogen, soil electrical conductivity, and pH. Nut. Cycl. A.